www.czasopisma.pan.pl PAN www.journals.pan.pl
Chemical and Process Engineering 2019, 40 (4), 361–376
DOI: 10.24425/cpe.2019.130212

Graphene oxide-based nanomaterials as catalysts for oxygen reduction reaction

Zuzanna Bojarska*, Marta Mazurkiewicz-Pawlicka, Łukasz Makowski

Faculty of Chemical and Process Engineering, Warsaw University of Technology, Warynskiego 1, 00-645 Warsaw, Poland

The aim of the presented research was to test different carbon supports, such as graphene oxide (GO), graphene oxide modified with ammonia (N-GO), and reduced graphene oxide (rGO) for catalysts used in a low-temperature fuel cell, specifically a proton exchange membrane fuel cell (PEMFC). Modification of the carbon supports should lead to different catalytic activity in the fuel cell. Reduction of GO leads to partial removal of oxygen groups from GO, forming rGO. Modification of GO with ammonia results in an enrichment of GO structure with nitrogen. A thorough analysis of the used supports was carried out, using various analytical techniques, such as FTIR spectroscopy and thermogravimetric (TGA) analysis. Palladium and platinum catalysts deposited on these supports were produced and used for the oxygen reduction reaction (ORR). Catalytic activity tests of the prepared catalysts were carried out in a home-made direct formic acid fuel cell (DFAFC). The tests showed that the enrichment of the GO structure with nitrogen caused an increase in the catalytic activity, especially for the palladium catalyst. However, reduction of GO resulted in catalysts with higher activity and the highest catalytic activity was demonstrated by Pt/rGO, because platinum is the most catalytically active metal for ORR. The obtained results may be significant for low-temperature fuel cell technology, because they show that a simple modification of a carbon support may lead to a significant increase of the catalyst activity. This could be useful especially in lowering the cost of fuel cells, which is an important factor, because thousands of fuel cells running on hydrogen are already in use in commercial vehicles, forklifts, and backup power units worldwide. Another method used for lowering the price of current fuel cells can involve developing new clean and cheap production methods of the fuel, i.e. hydrogen. One of them employs catalytic processes, where carbon materials can be also used as a support and it is necessary to know how they can influence catalytic activity.

Keywords: low-temperature fuel cells, carbon nanomaterials, oxygen reduction reaction, DFAFC

1. INTRODUCTION

The world is struggling with the problem of depletion of energy resources. The main sources of energy, such as coal, natural gas or petroleum are not renewable, and their use produces a lot of environmental pollution. There is also deep fear of using nuclear energy, therefore alternative technologies are sought (Bergstrom et al., 2011; Bilgen and Sarikaya, 2018; Dresselhaus and Thomas, 2001). Hydrogen is considered an ideal fuel for the future. Water-splitting is a promising way for clean, low-cost and environmentally friendly production of hydrogen, during which hydrogen evolution reaction (HER) occurs (Bae et al, 2017). Hydrogen produced in HER can be further used as a fuel for proton exchange membrane fuel cell (PEMFC). Hydrogen produced in the HER is pure and ideal for feeding it to the cell. The production of

* Corresponding author, e-mail: zuzanna.bojarska.dokt@pw.edu.pl

pure hydrogen in the process of water electrolysis and its use as a fuel could form the basis for sustainable and environmentally friendly energy industry (Bilgen and Sarikaya, 2018; Cano et al., 2018).

PEMFCs are an especially interesting alternative for the conventional energy sources because of their high efficiency of energy conversion, low operating temperature, and low emissions of pollutants (Akorede et al., 2010; Carrette et al., 2000; EG&G Technical Services, 2004). One type of PEM fuel cells is a direct formic acid fuel cell (DFAFC), in which liquid formic acid is fed as a fuel (Carrette et al., 2000; Rice et al., 2002; Yu and Pickup, 2008; Zhu et al., 2004). The advantages of DFAFCs over other low temperature fuel cells are: ability to obtain high power densities at lower temperatures, high electromotive force (1.45 V) and low permeability of formic acid through the Nafion®membrane (Rejal et al., 2014; Wang et al., 2004; Yu and Pickup, 2008; Zhu et al., 2004).

The most commonly used catalyst in DFAFC on the cathode side (where the oxygen reduction reaction - ORR occurs) is platinum. Due to very high price of platinum, the search for lower-cost alternatives has intensified (Gamburzev and Appleby, 2002; Rice et al., 2003; Shao et al., 2011). One alternative is to use a different metal, such as palladium which has a higher CO poisoning tolerance, which could lead to a longer lifetime of the fuel cell, resulting in lower cost. However, experimental studies show less activity in the oxygen reduction reaction than in platinum process (Antolini, 2009b; Jiang et al., 2014; Lesiak et al., 2016; Mazurkiewicz-Pawlicka et al., 2019; Mikolajczuk-Zychora et al., 2016; Tobes et al., 2001). Furthermore, in order to reduce the cost of catalysts and enhance catalytic activity, nanoparticle surface area can be increased, by using catalyst supports. Supports should have proper mechanical, thermal and electrical properties, high surface area, chemical indifference and stability in fuel cell working conditions (Antolini, 2009a; Sharma and Pollet, 2012). The most commonly used catalyst support for different reactions (such as ORR and HER) include carbon nanomaterials, such as graphene, reduced graphene oxide, and carbon nanotubes, due to their chemical and electrical properties (Antolini, 2009a; He and Que, 2016; Jung et al., 2008; Latorrata et al., 2018; Lesiak et al., 2016; Li et al., 2011; Mazurkiewicz-Pawlicka et al., 2019; Mikolajczuk-Zychora et al., 2016; Sharma and Pollet, 2012; Tobes et al., 2001).

Graphene oxide can be obtained by oxidization of graphite which leads to a large number of oxygen functional groups present in the carbon structure (Stobinski et al., 2014). On the one hand these groups decrease the electronic activity of the carbon support while on the other they can act as nucleation sites of catalyst nanoparticles (Compton and Nguyen, 2010; Zaaba et al., 2017). During catalyst preparation some functional groups are reduced and the conductivity of the support increases. Many nucleation sites in the support structure are responsible for better dispersion and production of smaller catalyst nanoparticles. Highly active surface of the catalysts is crucial for catalytic activity and thereby for the efficient production of electricity (Compton and Nguyen, 2010; Mayrhofer et al., 2008; Mazurkiewicz-Pawlicka et al., 2019; Seger and Kamat, 2009; Zaaba et al., 2017). As a result, it is possible to use graphene oxide as catalyst support (Gao et al., 2013; Seger and Kamat, 2009; Shin et al., 2009; Yang et al., 2011; Zhuo et al., 2013). To increase the conductivity of graphene oxide support reduction processes are often conducted (Gomez-Navarro et al., 2007) during which many functional groups are removed. Reduction of GO can decrease the number of nucleation sites resulting in worse dispersion and size increase of the catalyst particles. Aforementioned factors can influence the activity of prepared catalysts and it is necessary to compare which of these properties have higher significance for the catalyst effectiveness in fuel cells.

In addition, carbon nanomaterials can be modified by different functional groups (such as nitrogen/ sulfur/ boron-containing groups), which could enhance the catalytic efficiency of the obtained catalysts, due to the formation of more nucleation sites in the support structure or changing the electronic structure of the catalyst (Mazurkiewicz-Pawlicka et al., 2019; Puthusseri, and Ramaprabhu, 2016; Ratso et al., 2016; Su et al., 2013; Xu et al., 2014). According to Ratso et al. the presence of nitrogen groups (in particular pyridine) in the catalyst structure contribute to the increase of the activity for the ORR. Nitrogen-doped carbon materials were compared to commercial Pt/C catalyst and catalytic activity and stability were very

comparable (Ratso et al., 2016). Also, Su et al. (2013) reported that the enrichment of the graphene structure with nitrogen groups improved the catalytic activity of catalysts used for the ORR in alkaline conditions. According to Xu et al. (2014) boron-doped graphene and nitrogen-doped graphene calcined at 700 °C demonstrated excellent electrocatalytic oxygen reduction activity. Mazurkiewicz-Pawlicka et al. (2019) proposed a simple method using ammonia solution for enhancing the catalytic activity of Pd/MWCNT catalyst for formic acid electrooxidation. Based on these reports we proposed a functionalization of GO with nitrogen using an aqueous ammonia solution.

The aim of this work was comparison of different carbon supports, such as graphene oxide (GO), graphene oxide modified with ammonia (N-GO) and reduced graphene oxide (rGO) on the catalytic activity of Pd and Pt nanoparticles used for ORR in DFAFC. The obtained results can give information about which properties of the carbon support are crucial for the catalysts and can lead to future design of new materials with high activity used in low temperature fuel cells.

2. MATERIALS AND METHODS

2.1. Carbon nanomaterials

Graphene oxide was obtained from graphite powder using a modified Hummer's method. The oxidation of graphite powder was carried out using sulfuric acid and potassium permanganate in the presence of sodium nitrate. In addition, the mixture was treated with hydrogen peroxide. After the process, the obtained product was filtrated in a special filtration system with ceramic membranes and exfoliated with ultrasounds. The final product was in the form of an aqueous solution of graphene oxide (Jaworski et al., 2018; Stobinski et al., 2014).

Reduced graphene oxide was prepared by a chemical reduction method (Stobinski et al., 2014). To remove oxygen-containing functional groups from the structure, graphene oxide was boiled with 50% hydrazine solution in an alkaline environment, rinsed with distilled water and then dried. A graphite-colored powder was the final product of the production process.

In order to obtain graphene oxide modified with ammonia, graphene oxide (1.4 wt.% aqueous solution) was dispersed in ammonia solution in an ultrasonic bath for 15 minutes, followed by an ultrasonic homogenizer for the next 5 minutes. The obtained mixture was dried at 70 °C. The product was obtained in the form of a foil.

2.2. Catalysts for oxygen reduction reaction

In the present research palladium and platinum catalysts deposited on various carbon supports (GO, N-GO, rGO) were synthesized (assuming 20 wt.% metal content) by $NaBH_4$ reduction reaction method (Lesiak et al., 2016). Because graphene oxide flakes tend to agglomerate, carbon support suspensions were dispersed in distilled water (concentration of 150 mg of carbon in 250 ml of water) using a high-pressure homogenizer (Microfluidics M-110P) and then using an ultrasonic bath for the next 15 min. Subsequently, the precursor solutions (H_2PtCl_6, $PdCl_2$) were gradually added dropwise to the suspensions. In the case of the platinum catalysts, 0.979 g of H_2PtCl_6 (8 wt.% in H_2O by Sigma Aldrich) was added, and in the case of the palladium catalysts 1.263 g of $PdCl_2$ (5 wt.% in 10 wt.% HCl by Sigma Aldrich) was added. The pH of the solutions was raised to ~11, using 1M sodium hydroxide solution. The prepared suspensions were left on a magnetic stirrer for 30 min, and then a reducing agent (2.5 ml of 1 M $NaBH_4$) solution was added dropwise to every sample and left for another hour. Finally, the obtained solutions were washed several times to remove

impurities (using DI water and acetone) and filtered on a vacuum filtration system. The obtained products were left to dry at room temperature.

2.3. Characterization of carbon nanomaterials and catalysts

Physicochemical analysis of the obtained carbon nanomaterials: GO, N-GO, and rGO was carried out, using various analytical techniques. Fourier-transform infrared spectroscopy (FTIR) analysis was carried out using Nicolet iS10 spectrometer from Thermo Scientific in attenuated total reflection (ATR) mode on a diamond crystal. Thermogravimetric analysis (TGA) was conducted using TGA/DSC 3+ analyzer from Mettler Toledo. The analysis was carried out from 30 °C to 1000 °C with 10 °C/min heating rate in 30 ml/min air flow. Elemental analysis (CHNS) was carried out using Flash 2000 analyzer from Thermo Scientific. The carbon samples (around 1 mg) were placed in a furnace (960 °C) where oxygen was injected. This allowed to evaluate the C, H, N and S content in the samples.

The analysis of the obtained catalysts was carried out, using the following analytical techniques: X-ray fluorescence analysis (XRF) and scanning electron microscopy (SEM). A device from Epsilon 3XLE by PANalytical was used for the XRF analysis. Samples were analyzed in special containers with a diameter of 28 mm, in which the bottom was a film made of a permeable X-ray polymer (Mylar) with a thickness of 3.6 μm. Due to the minimum volume of samples, only catalysts based on rGO were analyzed with XRF techniques. Hitachi S5500 field emission scanning electron microscope (FE-SEM) with a resolution of 0.4 nm was used. The images obtained as a result of the SEM analysis were taken in two modes: in the secondary electron (SE) mode and the bright-field scanning transmission electron microscopy (BF-STEM) mode. The SE mode allowed to obtain information about the surface morphology of the sample, and the BF-STEM mode allowed to obtain information about the size of particles. Samples were prepared by applying a few drops of the catalyst suspension in acetone on the TEM copper grid with carbon film. Based on SEM images, particle size distributions of catalysts were calculated.

2.4. Measurements of catalytic activity

In order to prepare the cathodes for DFAFC, the prepared catalyst samples were dispersed into Nafion® Solution Dispersion – alcohol based 1100 EW at 5 wt.% (Du Pont) solution and distilled water in the ultrasonic bath for 15 minutes. The amount of catalyst used for the ink was determined on the assumption that the catalyst content would be 0.5 mg metal/cm^2 with 30 wt.% losses. The electrodes with a 5 cm^2 active area were prepared using a "direct-paint" technique applying a catalyst ink on the carbon cloth diffusion layer. Next, the electrodes were hot-pressed in the drier at 120 °C for 30 minutes. To prepare the anodes the same method was used for the commercial catalyst 60 wt.% Pd/Vulcan (Premetek) with the assumption that the catalyst content would be 1.5 mg metal/cm^2 with 30 wt.% losses.

Catalytic activity and stability tests of the obtained catalysts (Pt/GO, Pt/N-GO, Pt/rGO, Pd/GO, Pd/N-GO, Pd/rGO) were carried out in a prototype direct formic acid fuel cell with Nafion membrane as the electrolyte and with 3 M HCOOH (p.a., Chempur) (She et al., 2014) fed to the anode at a flow rate of 0.5 ml/min, and air supplied to the cathode with a flow rate of 1000 ml/min. During measurements, the fuel cell was kept on a hot plate to maintain constant temperature (30 °C), which was checked by a pyrometer. Stability tests were carried out at constant current (equal to the current for the highest power obtained for each catalyst) for 30 minutes, measuring the voltage drop. Scheme of the used measurement system is presented in Fig. 1.

The DFAFC was connected to a programmable power source, which could be controlled by a computer set and was connected to the data collection system, thanks to which it was possible to read changes in the current and voltage in the system.

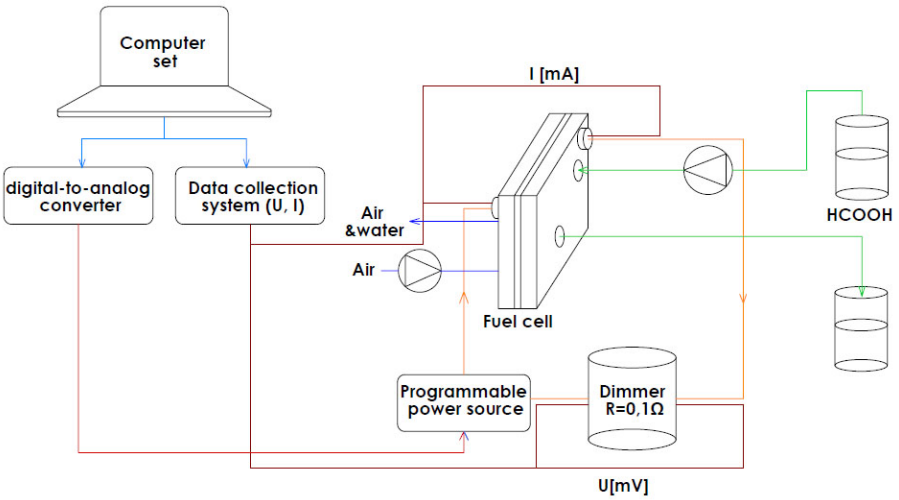

Fig. 1. Scheme of the used measurement system

3. RESULTS AND DISCUSSION

3.1. Characterization of carbon nanomaterials

Results obtained from the thermogravimetric analysis of carbon supports are shown in Fig. 2. TGA measurements showed differences in thermal stability of the analyzed carbon nanomaterials. It can be observed that graphene oxide shows the lowest thermal stability. Up to 100 °C, a small weight decrease is visible, which might be ascribed to water removal from GO. Another weight decrease is observed at around 200 °C, which might be due to thermal degradation of some functional groups present in GO. The biggest decrease is observed at ~450 °C suggesting the removal of other functional groups present in GO. For N-GO sample the TGA curve looks similar to GO. There is a smaller weight decrease up to 100 °C suggesting a smaller amount of water in the sample. Another difference is higher degradation temperature for N-GO. This result shows that the modification with ammonia resulted in small changes in GO structure, not leading to a reduction of the functional groups. TGA curve for rGO is significantly different from GO and N-GO samples. Only one weight decrease can be observed, and thermal stability of this material is the

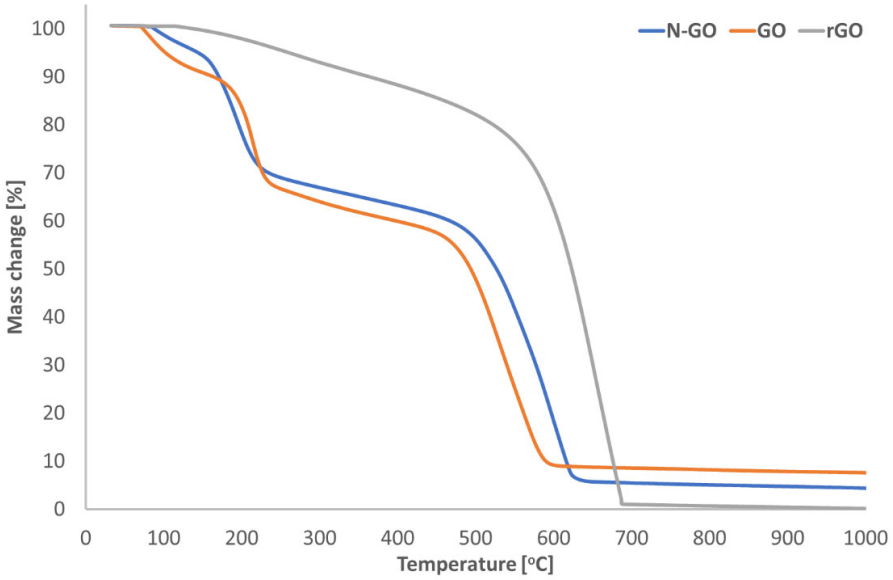

Fig. 2. Thermogravimetric analysis of carbon supports

highest compared to GO and N-GO. This result suggests that oxygen functional groups were removed (to a certain extent) from graphene oxide. According to the obtained data, the inorganic residue of rGO was the smallest and equaled 0 wt.%, while those of N-GO and GO were 4.24 wt.% and 7.46 wt.%, respectively. Inorganic impurities in the supports might be derived from the process of obtaining carbon materials.

Elemental analysis of carbon supports allowed to determine the contents of carbon, nitrogen, hydrogen, and sulfur in the samples. Based on the obtained data as a result of the elemental analysis and the TGA analysis, the oxygen content in the sample was estimated according to Equation (1):

$$C_O\ [\%] = 100\% - C_C - C_N - C_H - C_S - C_{TGA} \tag{1}$$

Results are presented in Table 1.

Table 1. Contents of C, H, N, S, O elements in carbon supports

	Carbon content [wt.%]	Nitrogen content [wt.%]	Hydrogen content [wt.%]	Sulphur content [wt.%]	TGA residue [wt.%]	Oxygen content [wt.%]
GO	48.98	0.00	2.18	1.03	7.46	40.35
N-GO	50.55	1.86	2.08	0.00	4.24	41.27
rGO	82.7	1.66	0.68	0.00	0.00	14.96

As can be seen, the reduction of GO led to partial removal of oxygen groups from GO. The content of oxygen in GO and in rGO was 14.96 wt.% and 40.35 wt.%, respectively. Modification of GO with ammonia resulted in an enrichment of the GO structure with nitrogen, up to 1.86 wt.%. In addition, due to ammonia modification, no reduction of oxygen groups was observed. The content of oxygen of N-GO was 41.27 wt.%. The presence of nitrogen in the rGO sample was the result of the use of hydrazine during the reduction process and in case of GO the presence of sulfur resulted from the use of sulfuric acid.

FTIR spectra of carbon supports are presented in Fig. 3. All tested carbon supports have shown characteristic absorption bands associated with carbonyl C=O stretching vibration (1710–1740 cm^{-1}) and C-O stretching vibration of alkoxy group (1050–1150 cm^{-1}). In case of GO and N-GO samples C–H deformation (around

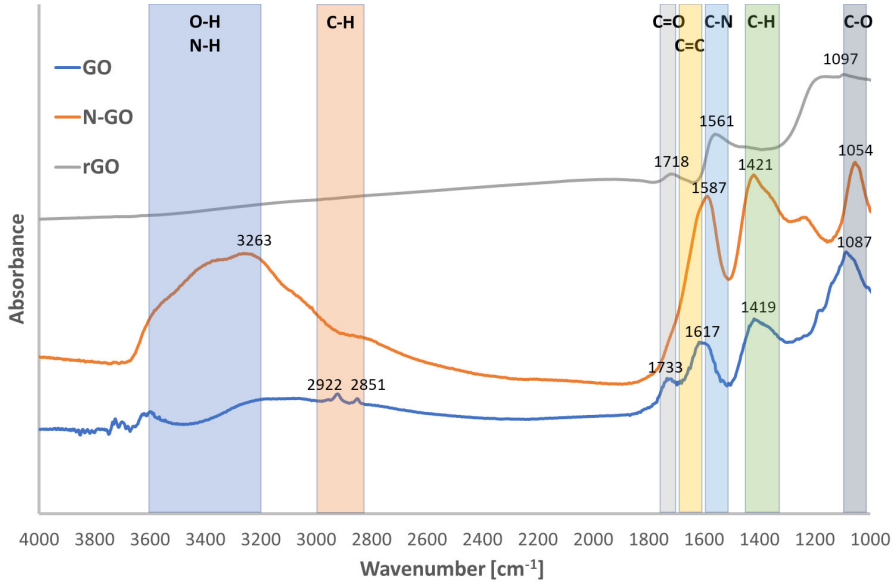

Fig. 3. FTIR analysis of carbon supports

1420 cm^{-1}), C=C stretching (about 1625 cm^{-1}), O–H stretching (3200–3600 cm^{-1}), and C–H stretching (2850–2960 cm^{-1}) could be also observed. Furthermore, in rGO and N-GO samples vibrations of the amide groups were observed (1530–1580 cm^{-1}). A highly intense band 3200–3600 cm^{-1} of the N-GO, corresponds to the presence of O–H (3200–3600 cm^{-1}) and N–H (3300–3500 cm^{-1}) functional groups within the structure. FTIR analysis confirmed the results from TGA and elemental analysis. The rGO sample was the most reduced carbon support (having the least functional groups, as evidenced by the smallest number of peaks), and the modification with ammonia resulted in a nitrogen enrichment of the GO sample.

3.2. Catalysts activity and stability in DFAFC

Results of the catalytic activity tests in the DFAFC of the synthesized catalysts are presented in Figs. 4–5.

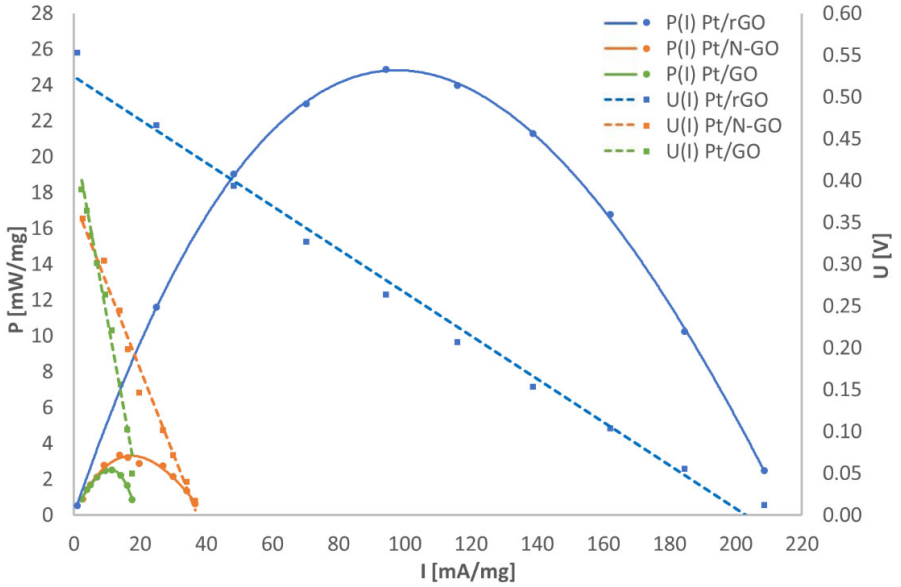

Fig. 4. The initial voltage and power density versus current density curves for platinum cathode catalysts (Pt/GO, Pt/N-GO, Pt/rGO) measured in DFAFC

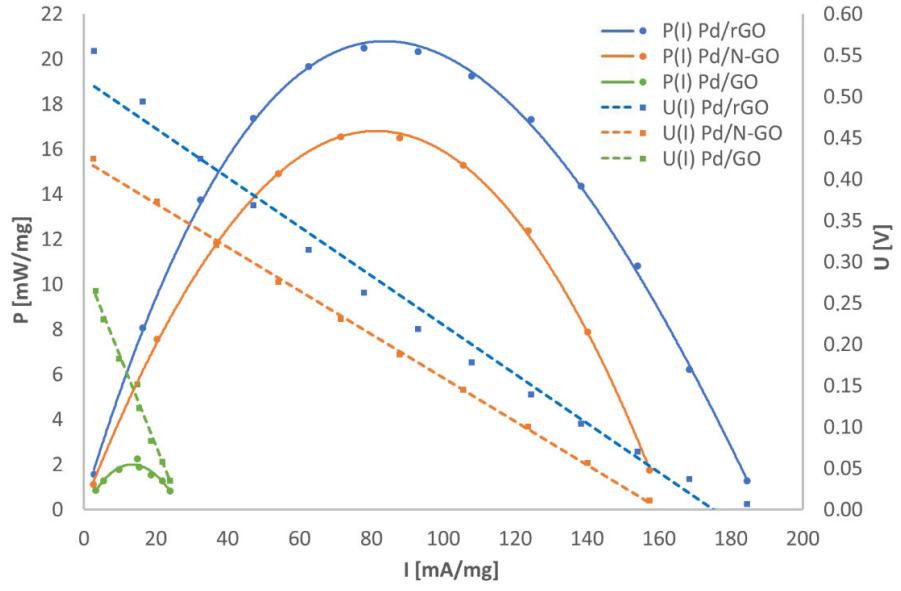

Fig. 5. The initial voltage and power density versus current density curves for palladium cathode catalysts (Pd/GO, Pd/N-GO, Pd/rGO) measured in DFAFC

The highest catalytic activity was demonstrated by the rGO-based catalysts. This might be due to the highest electron conductivity of reduced graphene oxide, but also the highest hydrophobicity. Both GO and N-GO still have many oxygen functional groups which make them very hydrophilic. High hydrophilicity can make the water produced during the work of the fuel cell not be removed from the catalyst surface. This might reduce the contact surface of oxygen with the catalyst and consequently decrease catalytic activity. The Pt/rGO catalyst allowed to obtain the highest fuel cell power density, equal to 24.9 mW/mg_{Pt}. This is because platinum is the most catalytically active metal for oxygen reduction reaction. Furthermore, the Pd/rGO catalyst allowed to obtain high fuel cell power density, equal to 20.5 mW/mg. The highest fuel cell power densities of the tested catalysts are presented in Table 2.

Table 2. The highest power densities of tested catalysts

Cathode	Highest power density [mW/mg_{metal}]
Pt/GO	2.5
Pd/GO	2.3
Pt/N-GO	3.4
Pd/N-GO	16.7
Pt/rGO	24.9
Pd/rGO	20.5

As can be seen from the results presented in Figs. 4–5 and Table 2, for each catalyst (Pt, Pd) supported on N-GO an increase in the catalytic activity is observed, compared to catalysts supported on GO. In the case of the Pd/N-GO catalyst, initial power density was equal to 16.7 mW/mg_{Pd} and was seven times higher in relation to the Pd/GO sample. These results suggest that enrichment of the carbon support with nitrogen can significantly enhance the catalytic activity of the catalyst.

The produced catalysts are stable, the loss of stability for each catalyst is less than 15% from the initial value (for 30 minutes). Catalysts based on palladium are more stable than platinum catalysts, which might suggest a better resistance to CO poisoning of Pd.

3.3. Catalyst characterization

XRF analysis allowed to estimate the contents of metals in the samples. Obtained results are presented in Table 3. As can be seen from results presented in Table 3, the actual content of the metal in the sample was around the assumed one (20 wt.%), suggesting a proper preparation method was used.

SEM images of produced catalysts are shown in Figs. 6–11. SEM results confirmed that the produced catalysts have nanometer sized particles. In the case of palladium catalysts, the Pd nanoparticles were evenly deposited on carbon supports, in particular in the Pd/N-GO sample (Fig. 9), which could contribute to the increase of their catalytic activity. Platinum catalysts, unfortunately, did not exhibit such an evenly distribution of particles and formed agglomerates, which could cause reduced activity of Pt catalysts. As can be seen in Fig. 6b and Fig. 7b Pt and Pd nanoparticles are not visible on the surface of the carbon flake, which can contribute to the worse catalytic activity of GO-supported samples compared to other produced catalysts.

Table 3. XRF analysis of the catalysts supported on rGO

Pt/rGO		Pd/rGO	
Element	Content [wt.%]	Element	Content [wt.%]
Cl	0.17	Pd	19.15
Pt	18.25	C*	80.85
C*	81.58		

* Content of elements such as C, O, H, N since it was not possible to distinguish these elements using XRF technique

a) b)

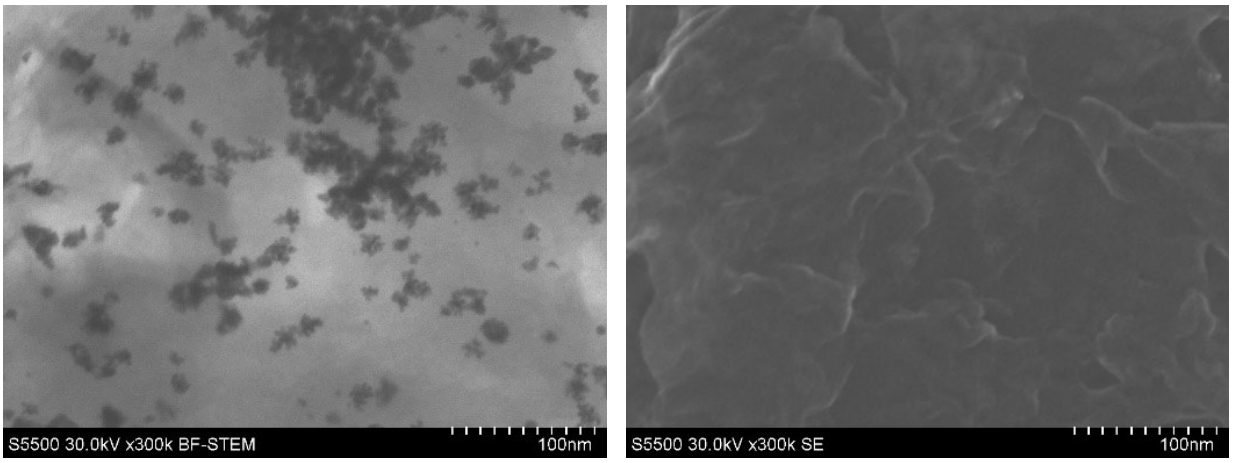

Fig. 6. SEM analysis of the Pt/GO; a) SE mode and on the right side; b) BF-STEM mode

a) b)

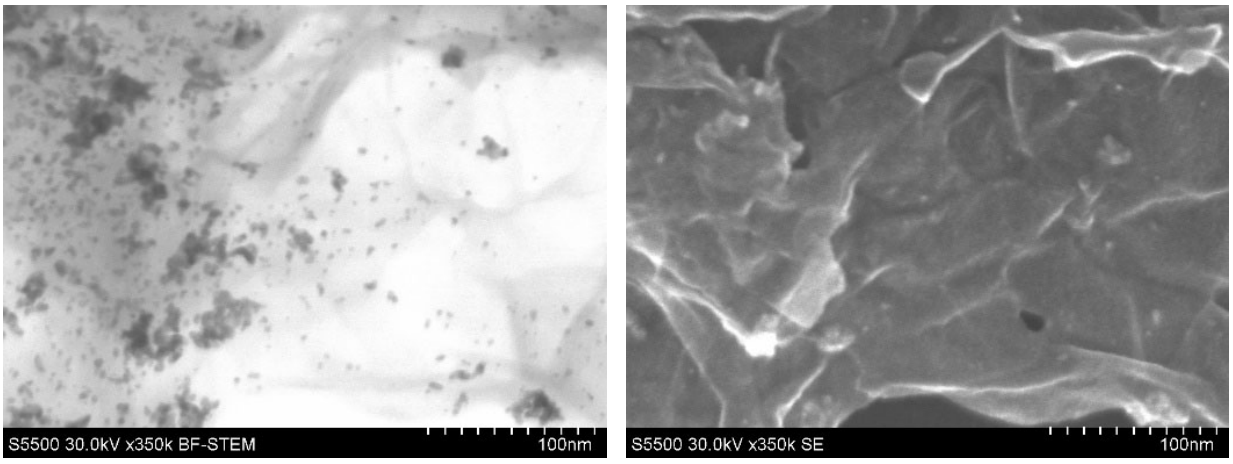

Fig. 7. SEM analysis of the Pd/GO; a) SE mode and on the right side; b) BF-STEM mode

Based on SEM images, particle size distributions of catalysts have been calculated (Fig. 12). Platinum catalysts form agglomerates, which can be seen in SEM images and particle size distributions. Especially Pt/rGO has bimodal particle size distribution with an average size of primary particle equal to 3.4 nm and average size of agglomerates equal to 20.4 nm. Palladium catalysts exhibit modal distributions with an average size of less than 5 nm for each sample.

a) b)

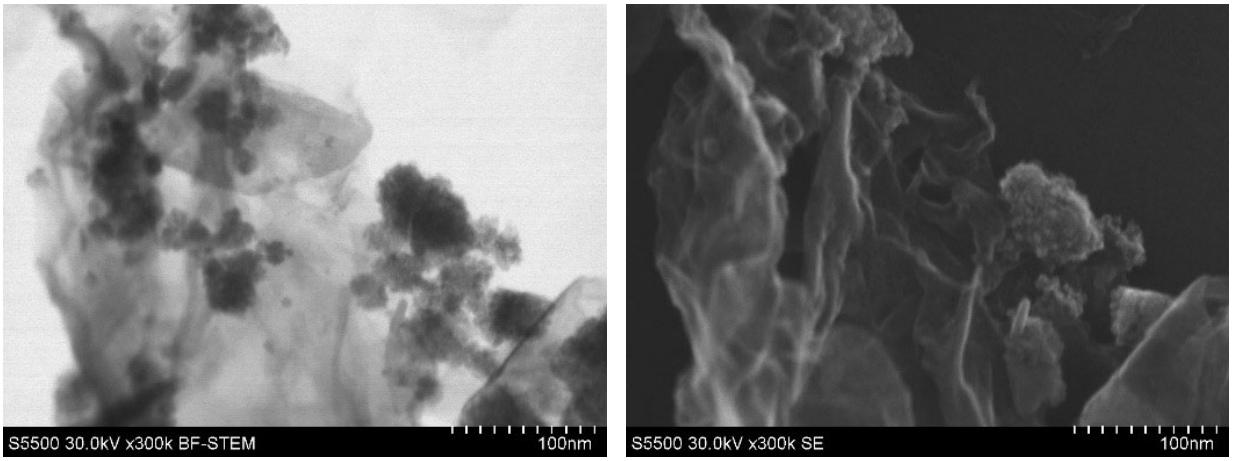

Fig. 8. SEM analysis of the Pt/N-GO; a) SE mode and on the right side; b) BF-STEM mode

a) b)

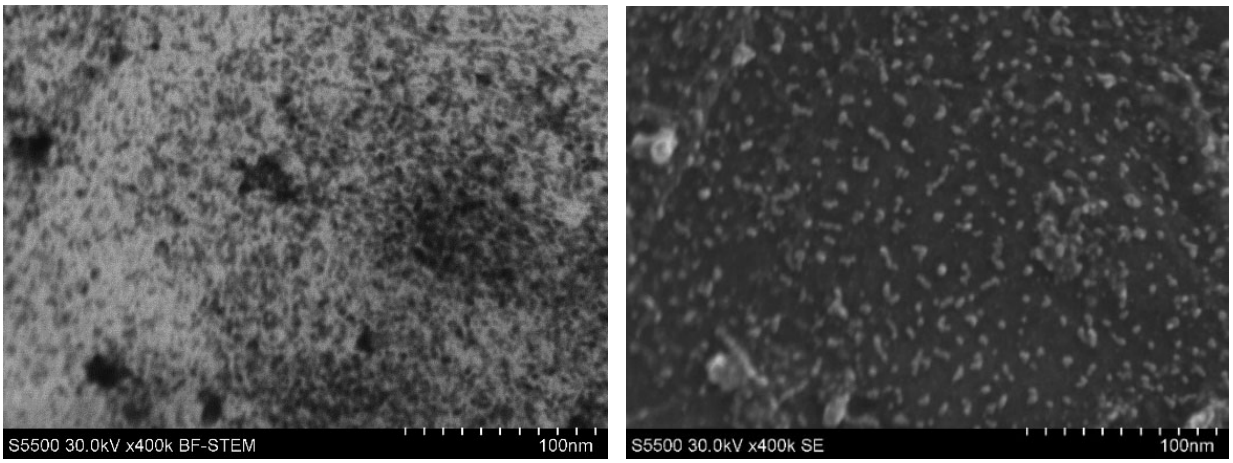

Fig. 9. SEM analysis of the Pd/N-GO; a) SE mode and on the right side; b) BF-STEM mode

a) b)

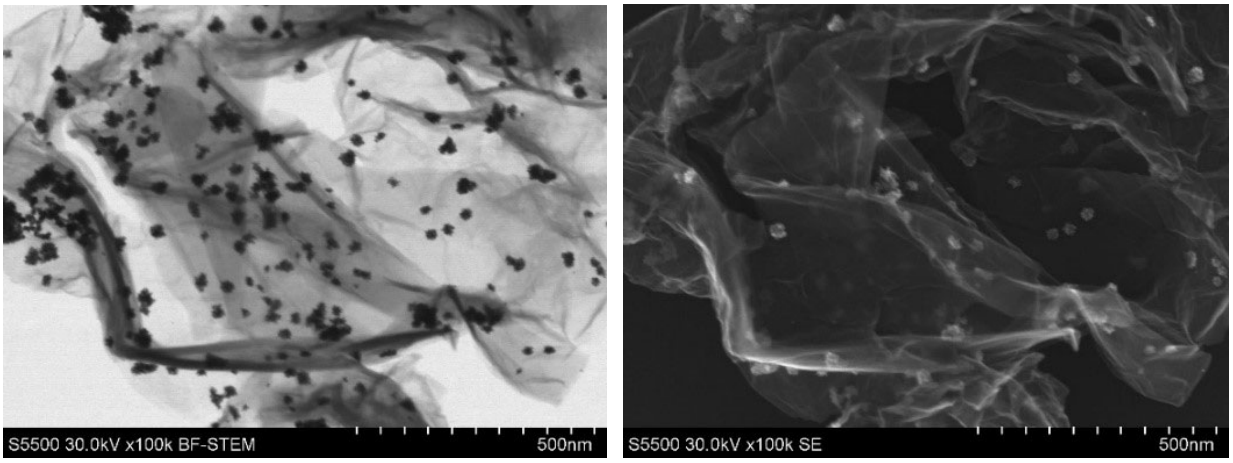

Fig. 10. SEM analysis of the Pt/rGO; a) SE mode and on the right side; b) BF-STEM mode

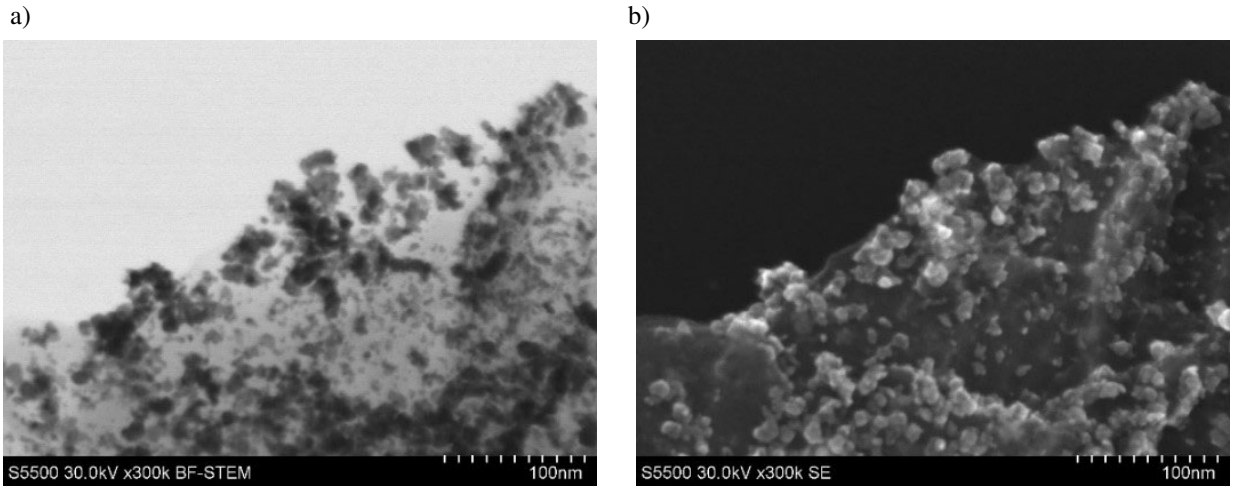

Fig. 11. SEM analysis of the Pd/rGO; a) SE mode and on the right side; b) BF-STEM mode

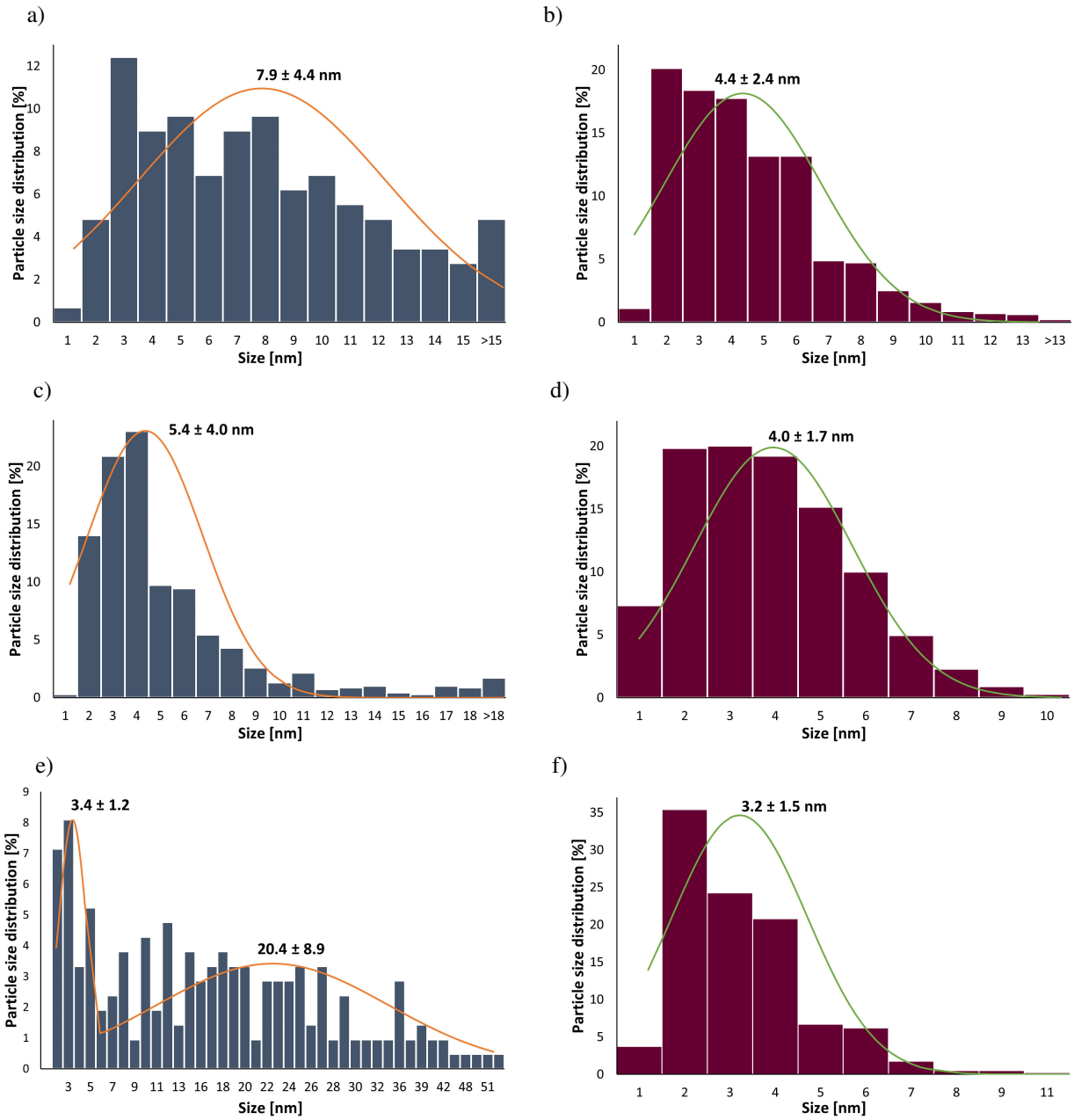

Fig. 12. Particle size distribution of (a) Pt/GO; (b) Pd/GO; (c) Pt/N-GO; (d) Pd/N-GO; (e) Pt/rGO; (f) Pd/rGO

4. CONCLUSIONS

Comparing the obtained results to literature data, it can be seen that in this paper much lower power densities were obtained. This is mainly due to the fact that measurements were performed in different conditions (e.g. air vs oxygen fed to the cathode side, different carbon supports tested). However, the advantage of the conducted experiments is the comparison of the work of many catalysts in identical operating conditions, which provides information about how different modifications of graphene oxide can influence the properties of the catalysts used for ORR in DFAFC. The best results were obtained for catalysts supported on rGO due to its highest electron conductivity and hydrophobicity compared to other tested materials. Pt/rGO catalyst exhibited the highest power density equal to 24.9 mW/mg_{Pt} which is due to the fact that platinum is the most catalytically active metal for oxygen reduction reaction. Enrichment of the GO structure with nitrogen resulted in an increase of the catalytic activity compared to GO (even seven-fold for Pd catalysts) due to higher dispersion and smaller particle size of the catalysts. The proposed modification method with ammonia solution is simple and low-cost and results in an increase of nitrogen up to 1.86 wt.% and does not significantly reduce the amount of oxygen functional groups present in the carbon structure. These results will be used in the future not only to better understand the catalytic properties of different materials used in low temperature fuel cells, but also to deliberately design fuel cell geometries to reduce unwanted phenomena such as the reduction of the active surface by residual water.

5. OUTLINE

Undoubtedly, fuel cells are considered to be a renewable and efficient method of energy production. For current low-temperature fuel cells, one of the primary fuels is hydrogen, which is called the green energy source of the future (Bergstrom et al., 2011; Carrette et al., 2000; Dresselhaus and Thomas, 2001). One of the methods of its production is water-splitting. It is a promising way for clean, low-cost and sustainable production of hydrogen. During water-splitting, hydrogen is produced by hydrogen evolution reaction (HER), which is presented by reaction (2):

$$2H_2O + 2e^- \leftrightarrow 2OH^- + H_2 \tag{2}$$

For HER, platinum, gold, and silver catalysts are known as the most effective. In order to commercialize fuel cells powered by hydrogen, cheaper catalysts to obtain hydrogen are sought (Hisatomi et al., 2014; Roger et al., 2017).

Molybdenum disulfide (MoS_2) seems to be a very promising catalyst for HER, which can be conducted in the photocatalytic or electrocatalytic process. MoS_2 has a crystal structure consisting of layers of S–Mo–S where a layer of molybdenum atom is sandwiched by two layers of sulfur atoms. MoS_2 is thought to be the most renowned H_2-evolution catalyst due to its low cost, excellent chemical stability, non-toxicity, and high reactivity (He and Que, 2016; Li et al., 2011; Yuan et al., 2015). The main method of obtaining molybdenum disulfide is its extraction from natural molybdenite. Unfortunately, as every fossil material – molybdenite shows varied properties depending on the source of origin and cleaning treatment process. It can be done through the proper synthesis of MoS_2 precipitation process. The recent years have seen a noticeable growth of interest in the use of jet reactors in practical solutions, in particular with regard to obtaining nanoparticles. Chemical processes in these reactors can be controlled by various parameters, such as geometry of the impingement zone, velocity of dosing fluid, initial concentrations of reagents, etc. A high energy dissipation occurs for impinging jets because the kinetic energy of each jet stream is converted into a turbulent- like motion through a collision and redirection of the flow in a very small volume. The process streams for mixing must pass through this region without bypassing (Makowski et

al., 2012; Wojtas et al., 2017). Literature already lists the first solutions of using jet-rectors to obtain nanoparticles of MoS_2 (Santillo et al., 2012).

As in the case of the catalysts for ORR, to improve the photocatalytic activity of MoS_2 carbon nanomaterials are used as the catalyst support (He and Que, 2016; Lei et al., 2013; Li et al., 2011; Yuan et al., 2015). Carbon supports enriched with nitrogen seem to be very promising as a support for catalysts based on MoS_2 for HER (He and Que, 2016; Lei et al., 2013). Hydrogen produced in hydrogen evolution reaction can be further used as a fuel in PEMFC. Nevertheless, the application of MoS_2 catalysts based on modified carbon supports needs further research.

This work was supported by the National Science Centre [No. 2017/27/B/ST8/01382] and by the National Centre for Research and Development [No.PL- TWIII/4/2016].

SYMBOLS

C_O	oxygen content, wt.%
C_C	carbon content, wt.%
C_N	nitrogen content, wt.%
C_H	hydrogen content, wt.%
C_S	sulfur content, wt.%
C_{TGA}	inorganic residue after TGA analysis, wt.%

REFERENCES

Akorede M.F., Hizam H., Pouresmaeil E., 2010. Distributed energy resources and benefits to the environment. *Renewable and Sustainable Energy Rev.*, 14, 724–734. DOI: 10.1016/j.rser.2009.10.025.

Antolini E., 2009a. Carbon supports for low-temperature fuel cell catalysts. *Appl. Catal. B Environ.*, 88, 1–24. DOI: 10.1016/j.apcatb.2008.09.030.

Antolini E., 2009b. Palladium in fuel cell catalysis. *Energy Environ. Sci.*, 2, 915–931. DOI: 10.1039/B820837A.

Bae D., Seger B., Vesborg P.C.K., Hansen O., Chorkendorff I., 2017. Strategies for stable water splitting: Via protected photoelectrodes. *Chem. Soc. Rev.*, 46, 1933–1954, DOI: 10.1039/C6CS00918B.

Bergstrom J. C., Randall A., 2011. *Resource economics: An economic approach to natural resource and environmental policy*. 4th ed., Edward Elgar Pub, Cheltenham.

Bilgen S., Sarikaya I., 2018. Energy conservation policy and environment for a clean and sustainable energy future. *Energy Sources Part B*, 13, 183–189. DOI: 10.1080/15567249.2017.1423412.

Cano Z.P., Banham D., Ye S., Hintennach A., Lu J., Fowler M., Chen Z., 2018. Batteries and fuel cells for emerging electric vehicle markets. *Nat. Energy*, 3, 279–289. DOI: 10.1038/s41560-018-0108-1.

Carrette L., Friedrich, K.A., Stimming U., 2000. Fuel cells: Principles, types, fuels, and applications. *Chem. Phys. Chem.*, 1, 162–193. DOI: 10.1002/1439-7641(20001215)1:4<162::AID-CPHC162>3.0.CO;2-Z.

Compton O.C., Nguyen S.T., 2010. Graphene oxide, highly reduced graphene oxide, and graphene: Versatile building for carbon-based materials. *Small*, 6, 711–723. DOI: 10.1002/smll.200901934.

Dresselhaus M.S., Thomas I.L., 2001. Alternative energy technologies. *Nature*, 414, 332–337. DOI: 10.1038/35104599.

EG&G Technical Services, Inc., 2004. *Fuel Cell Handbook*. Department of Energy. Office of Fossil Energy, National Energy Technology Laboratory, Morgantown.

Gamburzev S., Appleby A.J., 2002. Recent progress in performance improvement of the proton exchange membrane fuel cell (PEMFC). *J. Power Sources*, 107, 5–12. DOI: 10.1016/S0378-7753(01)00970-3.

Gao L., Yue W., Tao S., Fan L., 2013. Novel strategy for preparation of graphene-Pd, Pt composite, and its enhanced electrocatalytic activity for alcohol oxidation. *Langmuir*, 29, 957–964. DOI: 10.1021/la303663x.

Gomez-Navarro C., Weitz R.T., Bittner A.M., Scolari M., Mews A., Burghard M., Kern K., 2007. Electronic transport properties of individual chemically reduced graphene oxide sheets. *Nano Lett*., 7, 3499–3503. DOI: 10.1021/nl072090c.

He Z., Que W., 2016. Molybdenum disulfide nanomaterials: Structures, properties, synthesis and recent progress on hydrogen evolution reaction. *Appl. Mater. Today*, 3, 23–56. DOI: 10.1016/j.apmt.2016.02.001.

Hisatomi T., Kubota J., Domen K., 2014. Recent advances in semiconductors for photocatalytic and photoelectrochemical water splitting. *Chem. Soc. Rev*., 43, 7520–7535. DOI: 10.1039/C3CS60378D.

Jaworski S., Wierzbicki M., Sawosz E., Jung A., Gielerak G., Biernat J., Jaremek H., Łojkowski W., Woźniak B., Wojnarowicz J., Stobinski L., Malolepszy A., Mazurkiewicz M., Łojkowski M., Kurantowicz N., Chwalibog A., 2018. Graphene oxide-based nanocomposites decorated with silver nanoparticles as an antibacterial agent. *Nanoscale Res. Lett*., 13, 116. DOI: 10.1186/s11671-018-2533-2.

Jiang K., Zhang H.-X., Zou S., Cai W.-B., 2014. Electrocatalysis of formic acid on palladium and platinum surfaces: from fundamental mechanisms to fuel cell applications. *Phys. Chem. Chem. Phys*., 16, 20360–20376. DOI: 10.1039/C4CP03151B.

Jung I., Dikin D.A., Piner R.D., Ruoff R.S., 2008. Tunable electrical conductivity of individual graphene oxide sheets reduced at "low" temperatures. *Nano Lett*., 3, 4283–4287. DOI: 10.1021/nl8019938.

Latorrata S., Pelosato R., Stampino P.G., Cristiani C., Dotelli G., 2018. Use of electrochemical impedance spectroscopy for the evaluation of performance of PEM fuel cells based on carbon cloth gas diffusion electrodes. *J. Spectro.*, 1–13. DOI: 10.1155/2018/3254375.

Lei G., Changcun H., Xinlai X., Lele G., 2013. Synthesis and characterization of composite visible light active photocatalysts MoS_2 g-C_3N_4 with enhanced hydrogen evolution activity. *Int. J. Hydrog. Energy*, 38, 6960–6969. DOI: 10.1016/j.ijhydene.2013.04.006.

Lesiak B., Mazurkiewicz M., Malolepszy A., Stobinski L., Mierzwa B., Mikolajczuk-Zychora A.B., Juchniewicz K., Borodzinski A., Zemek J., Jiricek P., 2016. Effect of the Pd/MWCNTs anode catalysts preparation methods on their morphology and activity in a direct formic acid fuel cell. *Appl. Surf. Sci.*, 387, 929–937. DOI: 10.1016/j.apsusc.2016.06.152.

Li Y., Wang H., Xie L., Liang Y., Hong G., Dai H., 2011. MoS_2 nanoparticles grown on graphene: An advanced catalyst for the hydrogen evolution reaction. *Am. Chem. Soc*., 133, 7296–7299. DOI: 10.1021/ja201269b.

Makowski Ł., Orciuch W., Bałdyga J.R., 2012. Large eddy simulations of mixing effects on the course of precipitation process. *Chem. Eng. Sci*., 77, 85–94. DOI: 10.1016/j.ces.2011.12.020.

Mayrhofer K.J.J., Strmcnik D., Blizanac B.B., Stamenkovic V., Arenz M., Markovic N.M., 2008. Measurement of oxygen reduction activities via the rotating disc electrode method: From Pt model surfaces to carbon-supported high surface area catalysts. *Electrochim. Acta*, 53, 3181–3188. DOI: 10.1016/j.electacta.2007.11.057.

Mazurkiewicz-Pawlicka M., Malolepszy A., Mikolajczuk-Zychora A., Mierzwa B., Borodzinski A., Stobinski L., 2019. A simple method for enhancing the catalytic activity of Pd deposited on carbon nanotubes used in direct formic acid fuel cells. *Appl. Surf. Sci.*, 476, 806–814. DOI: 10.1016/j.apsusc.2019.01.114.

Mikolajczuk-Zychora A.B., Kedzierzawski P., Mierzwa B., Mazurkiewicz-Pawlicka M., Stobinski L., Ciecierska E., Zimoch E., Opałło M., 2016. Highly active carbon supported Pd cathode catalysts for direct formic acid fuel cells. *Appl. Surf. Sci.*, 199, 645–652. DOI: 10.1016/j.apsusc.2016.02.065.

Puthusseri G.D., Ramaprabhu S., 2016. Oxygen reduction reaction activity of platinum nanoparticles decorated nitrogen doped carbon in proton exchange membrane fuel cell under real operating conditions. *Int. J Hydrog. Energy*, 41, 13163–13170. DOI: 10.1016/j.ijhydene.2016.05.146.

Ratso S., Kruusenberg I., Joost U., Saar R., Tammeveski K., 2016. Enhanced oxygen reduction reaction activity of nitrogen-doped graphene/multi-walled carbon nanotube catalysts in alkaline media. *Int. J Hydrog. Energy*, 41, 22510–22519. DOI: 10.1016/j.ijhydene.2016.02.021.

Rejal S.Z., Masdar M.S., Kamarudin S.K., 2014. A parametric study of the direct formic acid fuel cell (DFAFC) performance and fuel crossover. *Int. J. Hydrog. Energy*, 39, 10267–10274. DOI: 10.1016/j.ijhydene.2014.04.149.

Rice C., Ha S., Masel R.I., Waszczuk P., Wieckowski A., Barnard T., 2002. Direct formic acid fuel cells. *J. Power Sour.*, 111, 1, 83–89. DOI: 10.1016/S0378-7753(02)00271-9.

Rice C., Ha S., Masel R.I., Wieckowski A., 2003. Catalysts for direct formic acid fuel cells. *J. Power Sour.*, 115, 2, 229–235. DOI: 10.1016/S0378-7753(03)00026-0.

Roger I., Shipman M.A., Symes M.D., 2017. Earth-abundant catalysts for electrochemical and photoelectrochemical water splitting. *Nat. Rev. Chem.*, 1, 0003. DOI: 10.1038/s41570-016-0003.

Santillo G., Deorsola F., Bensaid S., Russo N., Fino D., 2012. MoS_2 nanoparticle precipitation in turbulent micromixers. *Chem. Eng. J.*, 207–208, 322–328. DOI: 10.1016/j.cej.2012.06.127.

Seger B., Kamat P.V., 2009. Electrocatalytically active graphene-platinum nanocomposites. Role of 2-D carbon support in PEM fuel cells. *J. Phys. Chem. C*, 133, 7990–7995. DOI: 10.1021/jp900360k.

Shao M., Peles A., Shoemaker K., 2011. Electrocatalysis on platinum nanoparticles: Particle size effect on oxygen reduction reaction activity. *Nano Lett.*, 11, 3714–3719. DOI: 10.1021/nl2017459.

Sharma S., Pollet B.G., 2012. Support materials for PEMFC and DMFC electrocatalysts – A review. *J. Power Sour.*, 208, 96–119. DOI: 10.1016/j.jpowsour.2012.02.011.

She Y., Lu Z., Fan W., Jewell S., Leung M.K.H., 2014. Facile preparation of PdNi/rGO and its electrocatalytic performance towards formic acid oxidation. *J. Mater. Chem. A*, 2, 3894–3898. DOI: 10.1039/C3TA14546H.

Shin H.-J., Kim K.K., Benayad A., Yoon S.-M., Park H.K., Jung I.-S., Jin M.H., Jeong H.-K., Kim J.M., Choi J.-Y., Lee Y.H., 2009. Efficient reduction of graphite oxide by sodium borohydride and its effect on electrical conductance. *Adv. Funct. Mater.*, 19, 1987–1992. DOI: 10.1002/adfm.200900167.

Stobinski L., Lesiak B., Malolepszy A., Mazurkiewicz M., Mierzwa B., Zemek J., Jiricek P., Bieloshapka I., 2014. Gaphene oxide and reduced graphene oxide studied by the XRD, TEM and electron spectroscopy methods. *J. Electron. Spectrosc. Relat. Phenom.*, 195, 145–154. DOI: 10.1016/j.elspec.2014.07.003.

Su Y., Zhang Y., Zhuang X., Li S., Wu D., Zhang F., Feng X., 2013. Low-temperature synthesis of nitrogen/sulfur co-doped three-dimensional graphene frameworks as efficient metal-free electrocatalyst for oxygen reduction reaction. *Carbon*, 62, 296–301. DOI: 10.1016/j.carbon.2013.05.067.

Tobes M.L., van Dillen J.A., de Jong K.P., 2001. Synthesis of supported palladium catalysts. *J. Mol. Catal. A: Chem.*, 173, 75–98. DOI: 10.1016/S1381-1169(01)00146-7.

Wang X., Hu J.M., Hsing I.M., 2004. Electrochemical investigation of formic acid electro-oxidation and its crossover through a Nafion® membrane. *J. Electroanal. Chem.*, 562, 73–80. DOI: 10.1016/j.jelechem.2003.08.010.

Winter M., Brodd R.J., 2004. What are batteries, fuel cells, and supercapacitors? *Chem. Rev.*, 104, 4245–4270. DOI: 10.1021/cr020730k.

Wojtas K., Orciuch W., Makowski Ł., 2017. Modeling and experimental validation of subgrid scale scalar variance at high Schmidt numbers. *Chem. Eng. Res. Des.*, 123, 141–151. DOI:10.1016/j.cherd.2017.05.003.

Xu X., Yuan T., Zhou Y., Li Y., Lu J., Tian X., Wang D., Wang J., 2014. Facile synthesis of boron and nitrogen-doped graphene as efficient electrocatalyst for the oxygen reduction reaction in alkaline media. *Int. J. Hydrogen Energy*, 39, 16043–16052. DOI: 10.1016/j.ijhydene.2013.12.079.

Yang J., Tian C., Wanga L., Fu H., 2011. An effective strategy for small-sized and highly-dispersed palladium nanoparticles supported on graphene with excellent performance for formic acid oxidation. *J. Mater. Chem.*, 21, 3384–3390. DOI: 10.1039/C0JM03361H.

Yu X., Pickup P.G., 2008. Recent advances in direct formic acid fuel cells (DFAFC). *J. Power Sources*, 182, 124–132. DOI: 10.1016/j.jpowsour.2008.03.075.

Yuan Y.J., Lu H.W., Yu Z.T., Zou Z.G., 2015. Noble-metal-free molybdenum disulfide cocatalyst for photocatalytic hydrogen production. *Chem. Sus. Chem*., 8, 4113–4127. DOI: 10.1002/cssc.201501203.

Zaaba N.I., Foo K.L., Hashim U., Tan S.J., Liu W.-W., Voon C., 2017. Synthesis of graphene oxide using modified hummers method: Solvent influence. *Procedia Eng.*, 184, 469–477. DOI: 10.1016/j.proeng.2017.04.118.

Zhu Y., Ha S.Y., Masel R.I., 2004. High power density direct formic acid fuel cells. *J. Power Sources*, 130, 8–14. DOI: 10.1016/j.jpowsour.2003.11.051.

Zhuo Q., Gao J., Peng M., Bai L., Deng J., Xia Y., Ma Y., Zhong J., Sun X., 2013. Large-scale synthesis of graphene by the reduction of graphene oxide at room temperature using metal nanoparticles as catalyst. *Carbon*, 52, 559–564. DOI: 10.1016/j.carbon.2012.10.014.

Received 19 September 2019
Received in revised form 30 October 2019
Accepted 31 October 2019